

Cascade wide-angle Y-junction 1×16 optical power splitter based on silicon wire waveguides on silicon-on-insulator

S. H. Tao^{1,*}, Q. Fang¹, J. F. Song^{1,2}, M. B. Yu¹, G. Q. Lo¹, and D. L. Kwong¹

¹Institute of Microelectronics, A*STAR, 11 Science Park Road, Science Park II, Singapore 117685

²State Key Laboratory on Integrated Opto-Electronics, College of Electronic Science and Engineering, Jilin University, Changchun, People's Republic of China 130023

* Corresponding author: taosh@ime.a-star.edu.sg

Abstract: A 1×16 optical power splitter with wide splitting angle, uniform outputs, and low excess loss is demonstrated. The 1×16 splitter comprising cascaded 1×2 splitters with arc-shaped branching waveguides is fabricated on the silicon-on-insulator (SOI) substrate. The gap between the branching waveguides is widened in a short propagation length such that influences of etch residues and air voids in the gap on the optical power uniformity are reduced significantly. The measured power uniformity of the 1×16 splitter is better than 0.3 dB at wavelength of 1550 nm.

©2008 Optical Society of America

OCIS codes: (230.1360) Beam splitters; (250.5300) Photonic integrated circuits; (220.0220) Optical design and fabrication.

References and links

1. J. Gamet and G. Pandraud, "Ultralow-loss 1×8 splitter based on field matching Y junction," *IEEE Photon. Technol. Lett.* **16**, 2060-2062 (2004).
2. K. K. Chung, H. P. Chan, P. L. Chu, "A 1×4 polarization and wavelength independent optical power splitter based on a novel wide-angle low-loss Y-junction," *Opt. Commun.* **267**, 367-372 (2006).
3. Z. T. Wang, Z. C. Fan, J. S. Xia, S. W. Chen, and J. Z. Yu, "1x8 cascaded multimode interference splitter in silicon-on-insulator," *Jpn. J. Appl. Phys.* **43**, 5085-5087 (2004).
4. D. Taillaert, H. Chong, P. I. Borel, L. H. Frandsen, R. M. De La Rue, and R. Baets, "A Compact Two-Dimensional Grating Coupler Used as a Polarization Splitter," *IEEE Photon. Technol. Lett.* **15**, 1249-1251 (2003).
5. H. Fukuda, K. Yamada, T. Tsuchizawa, T. Watanabe, H. Shinojima, and S. Itabashi, "Ultrasmall polarization splitter based on silicon wire waveguides," *Opt. Express* **14**, 12401-12408 (2006).
6. S. L. H. Frandsen, P. I. Borel, Y. X. Zhuang, A. Harpøth, M. Thorhauge, and M. Kristensen, "Ultralow-loss 3-dB photonic crystal waveguide splitter," *Opt. Lett.* **29**, 1623-1625 (2004).
7. Ch. Schuller, S. Höfling, A. Forchel, C. Etrich, T. Pertsch, R. Iliew, F. Lederer, and J. P. Reithmaier, "Highly efficient and compact photonic wire splitters on GaAs," *Appl. Phys. Lett.* **91**, 221102 (2007).
8. Y. A. Vlasov and S. J. McNab, "Losses in single-mode silicon-on-insulator strip waveguides and bends," *Opt. Express* **12**, 1622 (2004).
9. M. Olivero and M. Svalgaard, "UV-written Integrated Optical $1 \times N$ Splitters," *Opt. Express* **14**, 162-170 (2006).
10. W. Bogaerts, D. Taillaert, P. Dumon, D. Van Thourhout, R. Baets, and E. Pluk, "A polarization-diversity wavelength duplexer circuit in silicon-on-insulator photonic wires," *Opt. Express* **15**, 1567-1578 (2007).

1. Introduction

Silicon photonics has become an important area of research and development in the realization of micro- and nano-meter-scale optoelectronic devices. As silicon photonic devices can be made ultra compact with small bending radius, silicon-on-insulator (SOI) devices fabricated with the standard complementary metal oxide semiconductor (CMOS) technology are pursued highly in applications of broadband communication, high speed computation, and high resolution sensing. Splitters are one of the fundamental building elements for scaling high-density photonic integrated circuits (PIC) and are used as optical power dividers, combiners, attenuators, and routers. High performance splitters are key to the realization of an efficient PIC on a chip. Power uniformity and excess loss are the most important and critical

aspects for a splitter. The power uniformity is defined as the ratio of the maximum and minimum output powers, and the excess loss is the total loss induced by mode conversion and coupling in beam splitting. Various splitters based on Y-junction, multi-mode interference (MMI), grating, directional coupler, and photonic crystal have been reported [1-6]. Among them, Y-junction splitters are widely used, as they are insensitive to varying refractive index and can be realized with simple designs. However, a typical loss figure for a conventional Y-junction splitter is 1 dB with splitting angle of 1° [2]. With such a small angle, the gap is narrower than $0.5 \mu\text{m}$ in the waveguide length of about $30 \mu\text{m}$. Consequently, photo-resists or etch residues could be left in the gap or attached to branching waveguides during the fabrication processes. Air voids are also likely generated in a plasma-enhanced chemical vapor deposition process (PECVD) in the cladding of the etched splitter when the gap between branching waveguides is less than $2 \mu\text{m}$ [1]. Both the residues and air voids in a narrow gap would affect the power uniformity of the output ports and induce remarkable excess loss. To remedy the problem, researchers have used field matching method in a 1×8 splitter [1]. As the splitter is fabricated on silica materials instead of SOI, the device is relatively large in size. Moreover, a lower index material, added in the narrow gap region before a cladding layer has been deposited, makes the fabrication complicated. Recently, Schuller et al. [7] have demonstrated highly efficient and compact wire splitters using miniaturized 90° bends. They obtained a total excess loss of 8.4 dB for 6 cascades of a 1×6 T-splitter [7]. The 1×6 T-splitter was deliberately designed to output six uneven optical powers and was fabricated on GaAs, which was not compatible with the standard CMOS technology.

In this letter we will use the design similar to the T-splitter and demonstrate a compact 1×16 splitter fabricated on the SOI substrate. We use arc-shaped waveguides to replace the straight branching waveguides in the Y-junction region, so the splitting angle of the splitter can be as large as $\sim 52^\circ$. Chances of etch residues or air voids remained in the narrow region between two branching waveguides will be decreased, as the gap widens in a short propagation distance. Thus, the optical powers of the 16 outputs are expected to be uniform.

2. Simulation and experiment

2.1 Design and simulation

A conventional 1×2^N splitter can be realized with $2^N - 1$ 1×2 Y-junction splitters. In the Y-junction, the input waveguide is split into two branching waveguides with gradually widened gap. Since the branching waveguides should be strictly symmetric for mode coupling and conversion, etch residues or air voids in the junction region will break the symmetry and deteriorate the power uniformity. Furthermore, a flaw of the same size in a gap would have more significant effect on the power uniformity than that in a wider gap. To verify the influence of an air void in the gap of a conventional Y-splitter on the power uniformity, we employ a finite-difference time-domain method to analyze the light propagations. For simplicity, an air cylinder is used as air void in the simulation. The 1×2 Y-splitter in the simulation is cladded with silicon dioxide. The splitting angle is set as 4° and the cross-section of the waveguide is $500 \text{ nm} \times 200 \text{ nm}$. The radius of the air cylinder is set as 300 nm and it is positioned in the gap of the junction. Figure 1 displays the three-dimensional plot of the power uniformity of the outputs as a function of coordinates of the cylinder in the gap. The X axis and Y axis represent the horizontal and vertical positions of the cylinder in the gap, respectively. The center of the gap closest to the junction is set as the origin of the coordinate. In Fig. 1 the lower the grid, the better the uniformity of the splitter is. The simulation shows that the power uniformity deteriorates when the cylinder moves horizontally away from the symmetric center of the gap, and also deteriorates when the cylinder is not in the symmetric center and moves vertically towards the junction.

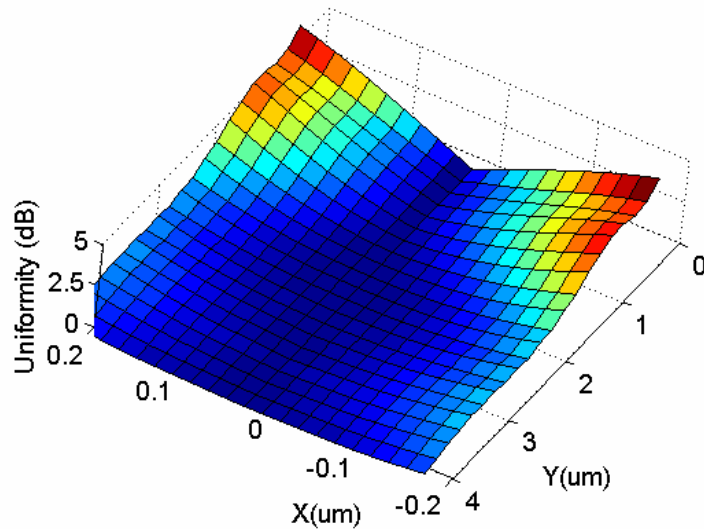


Fig. 1. Power uniformity of the outputs versus coordinates of the cylinder in the gap. The X axis and Y axis represent the horizontal and vertical positions of the cylinder.

To address the problem caused by unwanted residues and air voids, we use two identical arc-shaped waveguides to replace the linear branching waveguides in the junction region. In this way, the two arc-shaped branching waveguides will split wide in a short propagation distance. Thus, chances for imperfections remained in the gap would be lowered significantly. The split lights can propagate efficiently in the bent waveguides, as the bending loss for a typical SOI wire bend with radius larger than $5\ \mu\text{m}$ is negligible [8]. Obviously, the arcs with smaller radii will form a wider splitting angle, and vice versa. The splitting angle is calculated as the figure formed by two diverging branching waveguides that separate $2\ \mu\text{m}$ from each other. The branching waveguides can be regarded as linear before the gap width reaches to $2\ \mu\text{m}$. The splitting angle is about 52° when the bend radius is $5\ \mu\text{m}$. The schematic drawing of a 1×2 arc-shaped splitter is illustrated in Fig. 2(a).

2.2 Fabrication

In order to verify the performance of the arc-shaped splitter, we have fabricated a group of splitters of 1×2 , 1×4 , 1×8 , and 1×16 . We start the fabrication with deep UV 248 nm-stepping lithography process on an 8-inch SOI wafer. Then, we etch the pattern on the silicon core layer down to the buried silicon dioxide with inductively coupled plasma etch system, and clean the wafer with diluted HF and sulfuric acid-hydrogen peroxide mixture solutions. Finally, we deposit a layer of $3\ \mu\text{m}$ -thick silicon dioxide on the wafer with PECVD. The radii of the arcs vary from $5\ \mu\text{m}$ to $40\ \mu\text{m}$, and the cross-section of the waveguides is $500\ \text{nm} \times 200\ \text{nm}$. The refractive index difference between the silicon and the silicon dioxide is ~ 2 . Full length of each splitter is $3\ \text{mm}$, which also includes tapered waveguides for efficient coupling between the input or output ports of the splitters and the fibers. The tip width and length of the tapered waveguides are $150\ \text{nm}$ and $200\ \mu\text{m}$, respectively. The thicknesses of the buried silicon dioxide, the silicon core layer, and the top cladding of silicon dioxide are $2\ \mu\text{m}$, $200\ \text{nm}$, and $3\ \mu\text{m}$, respectively. A microscope picture of an arc-shaped 1×16 splitter is shown in Fig. 2(b). It should be noted that the waveguides connecting the arc-branching junctions are not necessarily in arcs or semicircles as shown in Fig. 2(b). The branching arcs can be connected directly with S-bends. The radii of the S-bends should be greater than $5\ \mu\text{m}$ for avoiding significant bending loss. Thus, the width of the splitter can be decreased by 50%. Currently, the chip size is $\sim 600\ \mu\text{m} \times 3000\ \mu\text{m}$. It is worth mentioning that the $3000\ \mu\text{m}$ includes total lengths of $400\ \mu\text{m}$ of inverse tapers, $\sim 800\ \mu\text{m}$ of input and output waveguides,

and $>1500\ \mu\text{m}$ of connecting waveguides between the cascades. The average length of the straight waveguides connecting the four cascades is greater than $500\ \mu\text{m}$, which can be shortened to $50\ \mu\text{m}$ without affecting the performance of the splitter. Hence, the total length of the four cascades of the 1×16 splitter can be decreased to $\sim 300\ \mu\text{m}$. The radii for the 1×16 splitter from the bottom to the top are $40\ \mu\text{m}$, $20\ \mu\text{m}$, $10\ \mu\text{m}$, and $5\ \mu\text{m}$, respectively, the radii for the 1×8 splitter are $20\ \mu\text{m}$, $10\ \mu\text{m}$, and $5\ \mu\text{m}$, respectively, and so on for the splitters 1×4 and 1×2 . The radii are chosen just for the convenience of the layout drawing. Two zoomed junctions with radii of $20\ \mu\text{m}$ and $5\ \mu\text{m}$ are displayed in Figs. 2(c) and 2(d), respectively. One can observe that the branching waveguides separate from each other widely in the length of only a few micrometers. The measured splitting angles range from about 15° to 52° . All the gaps are found free of remains.

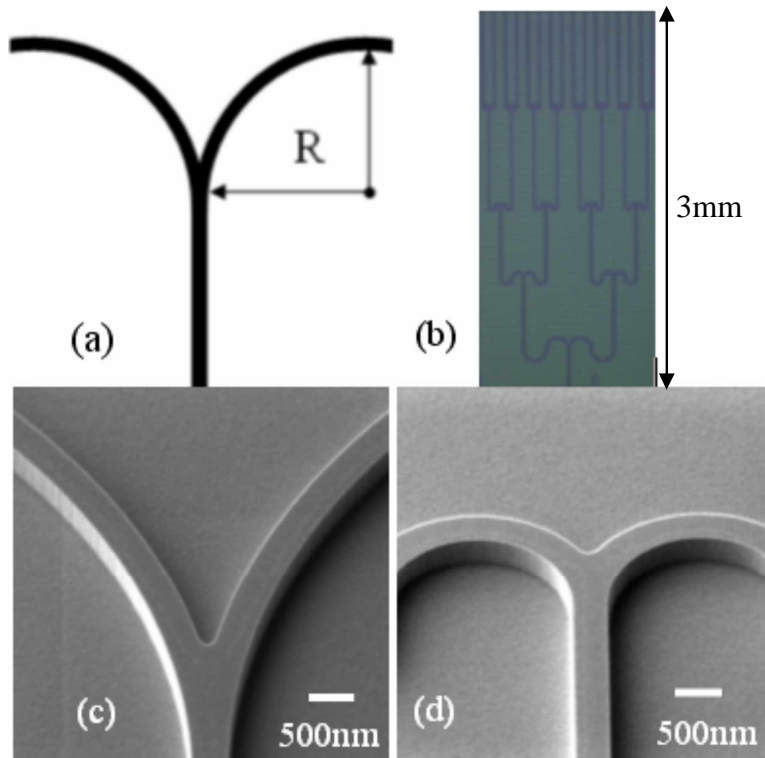


Fig. 2. (a). Schematic drawing of an arc-shaped Y-junction, (b) microscope picture of the 1×16 splitter, (c) fabricated arc-shaped Y-junction with arc radius of $20\ \mu\text{m}$, and (d) fabricated arc-shaped Y-junction with arc radius of $5\ \mu\text{m}$.

3. Characterization and results

In the characterization setup, we use lensed polarization maintaining fibers to end-fire couple the light in or out of the splitters. The diameter of the focused spot of the fiber is $\sim 2.5\ \mu\text{m}$. The facets at both ends of the splitters have been polished to improve coupling. A tunable laser is used as the input and a power meter is used for detecting the output power at $1550\ \text{nm}$. We also utilize a tunable laser and power meter, whose wavelength ranges from $1510\ \text{nm}$ to $1610\ \text{nm}$ with scanning step of $40\ \text{nm}$, to test the transmission spectra of the splitters. The splitter under testing is placed on a high-precision 3-axis automatic stage for alignment. The measured propagation loss and coupling loss for a straight waveguide are about $4.2\ \text{dB/cm}$ and $2.8\ \text{dB/facet}$, respectively. The propagation loss can be decreased by using oxidation to smooth the sidewalls of the waveguides. The measured insertion losses for the splitters of 1×2 , 1×4 , 1×8 , and 1×16 are plotted in Fig. 3(a). It is worth mentioning that the insertion loss

includes the coupling losses, the excess loss, and the propagation loss. All the insertion losses presented in Fig. 3(a) are the best values obtained in the measurement. We have also captured the output profiles of the splitters using an infrared camera. The captured output profiles for the splitters of 1×2 , 1×4 , 1×8 , and 1×16 are shown in Fig. 3(b), correspondingly. It can be seen that the brightness scales of the captured output modes of each group are nearly uniform.

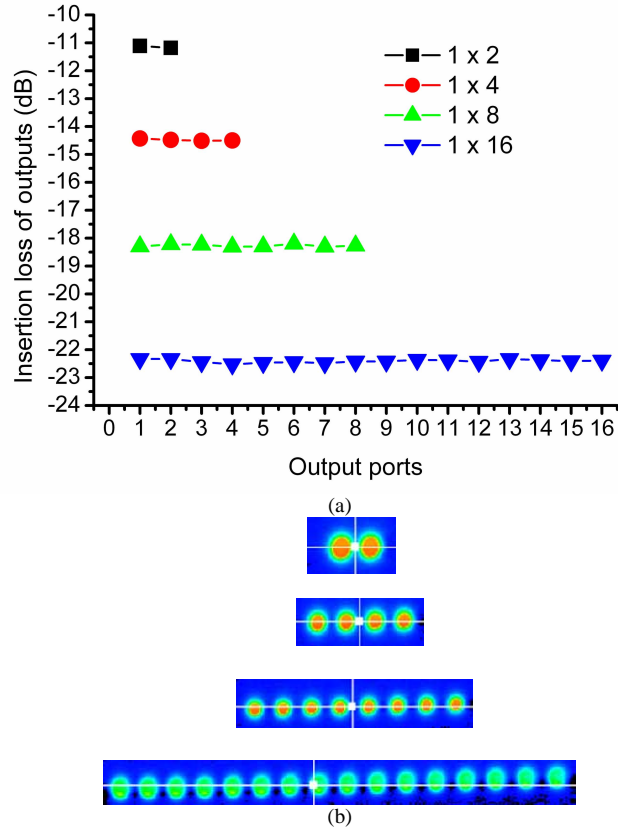


Fig. 3. (a). Insertion losses for the splitters of 1×2 , 1×4 , 1×8 , and 1×16 (from top to bottom), respectively, and (b) the corresponding output profiles.

The performances of the splitters at wavelength of 1550 nm are summarized in Table 1. It can be observed from Table 1 and Fig. 3 that the splitters have very uniform outputs. The measured output uniformities are better than 0.1 dB for a 1×2 splitter and better than 0.3 dB for a 1×16 splitter. The excess losses are 0.15 dB and 2.41 dB for the full devices, respectively. Note that the excess losses in the table exclude the propagation loss of the waveguides. Thus, the 1×16 splitter has about 0.6 dB excess loss per cascade. In Table 1 the quite larger increase of the total excess loss for the splitters with more cascades might be caused by the branching arcs with different radii used in different cascades, as the excess loss would not be the same for junctions with different branching arcs. Different excess losses were also incurred for splitting junctions with different splitting angles on a 1×32 S-bend silica-on-silicon splitter reported in [9]. We can use the same radius for all the branching arcs to get uniform excess losses. The arc radius can be optimized for decreasing the excess loss further. We also randomly choose three output ports of the 1×16 splitter and measure their transmission spectral, as shown in Fig. 4. For comparison, the spectrum of the 3-mm-long straight waveguide is also shown in Fig. 4. One can see that the transmission spectra of both devices have similar profile in the bandwidth of 100 nm. However, the splitter has more

obvious fluctuations, which may result from the polarization dependence. The measured polarization dependent loss (PDL) at wavelength of 1550 nm for the 1×16 splitter is greater than 5 dB. The high PDL is due to the limitation of the waveguide geometry, which favors TE (transverse electric) mode. We can adopt square cross section such as $300 \text{ nm} \times 300 \text{ nm}$ for the waveguides to decrease the PDL of the splitters. Alternatively, the splitters can be used for lights with favored polarization states only by adopting the polarization diversity scheme [10].

Table 1. Performances of the arc-shaped splitters.

Splitter	Uniformity (dB)	Excess loss (dB)
1×2	0.07	0.15
1×4	0.09	0.48
1×8	0.11	1.28
1×16	0.27	2.41

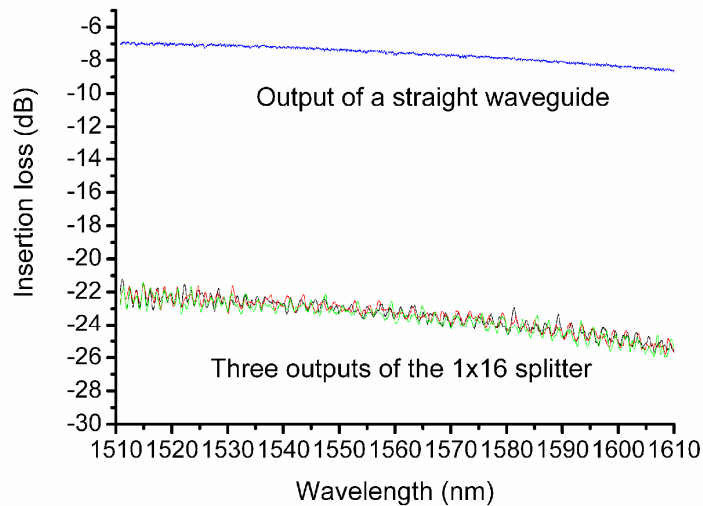


Fig. 4. Transmission spectra of three randomly chosen outputs of the 1×16 splitter and a straight waveguide.

4. Conclusion

In summary, arc-shaped branching waveguides are used to realize a 1×16 cascade splitter with wide splitting angle, uniform outputs, and low excess loss. The simulations show that an air void in the long and narrow gap of branching waveguides of a conventional Y-splitter would affect the output power uniformity significantly. As the arc-shaped branching waveguides are used to form a short and wide gap, the optical power uniformity improves significantly. The measured optical power uniformity is as good as 0.27 dB for the 1×16 splitter. The splitter is fabricated with the standard CMOS technology and would be useful for building large-scale photonic integrated circuits.